Methodological Overview (eds Gottlieb, G. & Krasnegor, N. A.) 253–300 (Westport, Connecticut, Ablex, 1985).

23. Baillargeon, R. in *Advances in Infancy Research* (ed. Lipsitt, C. R.-C. L. P.) 305–371 (Ablex, Norwood, 1995).

24. Hauser, M., Chomsky, N. & Fitch, W. T. The faculty of language: What is it, who has it, and how did it evolve? *Science* **298**, 1569–1579 (2002).

25. Werker, J. F. in *An Invitation to Cognitive Science* (eds Gleitman, L. & Liberman, M.) 87–106 (MIT, Cambridge, 1995).

....

Comparison of population coherence of place cells in hippocampal subfields CA1 and CA3

Inah Lee[*], **D. Yoganarasimha, Geeta Rao & James J. Knierim**

Department of Neurobiology and Anatomy, W.M. Keck Center for the Neurobiology of Learning and Memory, University of Texas Medical School at Houston, PO Box 20708, Houston, Texas 77225, USA

[*] Present address: Center for Memory and Brain, Boston University, 2 Cummington Street, Boston, Massachusetts 02215, USA

....

The hippocampus, a critical brain structure for navigation, context-dependent learning and episodic memory[1–3], is composed of anatomically heterogeneous subregions. These regions differ in their anatomical inputs as well as in their internal circuitry[4]. A major feature of the CA3 region is its recurrent collateral circuitry, by which the CA3 pyramidal cells make excitatory synaptic contacts on each other[4,5]. In contrast, pyramidal cells in the CA1 region are not extensively interconnected[4]. Although these differences have inspired numerous theoretical models of differential processing capacities of these two regions[6–13], there have been few reports of robust differences in the firing properties of CA1 and CA3 neurons in behaving animals. The most extensively studied of these properties is the spatially selective firing of hippocampal 'place cells'[1,14]. Here we report that in a dynamically changing environment, in which familiar landmarks on the behavioural track and along the wall are rotated relative to each other[15,16], the population representation of the environment is more coherent between the original and cue-altered environments in CA3 than in CA1. These results demonstrate a functional heterogeneity between the place cells of CA3 and CA1 at the level of neural population representations.

Five rats implanted with multiple recording probes in CA3 and CA1 were trained to circle clockwise (CW) on a circular track in a controlled, stable environment ('standard session'; STD in Fig. 1). Twelve tetrodes were lowered to CA3 and 6 tetrodes were lowered to CA1 (Fig. 2b). On each day of recording, three standard sessions were interleaved with two mismatch (MIS in Fig. 1) sessions, in which the local cues on the circular track were rotated anticlockwise (ACW) and the set of distal cues was rotated clockwise (CW) by an equal amount (Fig. 1). Total mismatch angles between the local and distal cue sets varied between 45°, 90°, 135° or 180°, and each rat received 4 sets of each rotation mismatch over 8 days.

Approximately 36% of the complex spike cells in CA1 (range 26–62%) and 26% of the complex spike cells in CA3 (range 22–33%) had place fields in the first standard session of the day; other cells were isolated in pre-session sleep periods but were silent or fired sparsely with no spatial selectivity. To first describe the heterogeneity of single-unit responses to the cue rotations, we categorized the individual place field responses into 5 groups (Fig. 2a). In some cases, the place cells rotated their preferred firing locations either CW or ACW, following in the direction of the distal or local cue sets, respectively. In other cases, place fields in standard sessions disappeared in mismatch sessions ('Disappear') or appeared only in the mismatch sessions ('Appear'). Some place fields could not be decisively categorized into the 4 response types described above, and were categorized as 'Ambiguous' (for example, when a cell had a single place field in one session and multiple place fields in the other session).

There were notable differences between CA1 and CA3 in the proportions of response types (Fig. 2c; $\chi^2 = 130.8$, $P < 0.0001$). The majority of CA3 place fields (~60%) rotated on the track (ACW, $n = 221/429$; CW, $n = 33/429$), whereas only ~27% of CA1 cells responded similarly (ACW, $n = 50/349$; CW, $n = 45/349$). In contrast, most CA1 cells altered their place fields (~73%), either showing ambiguous responses ($n = 128/349$) to the changed environments or having a robust place field in only one of the two sessions (Disappear, 98/349; Appear, 28/349). Only ~40% of CA3 cells altered their place fields in these ways. These general patterns between CA1 and CA3 were observed across all rats (Supplementary Fig. 1).

To validate objectively the categorical analysis described above, a population correlation analysis was performed. The firing rate of each cell was calculated for each 1° bin of the track, thus constructing a population firing rate vector for each of the 360 bins. The firing rate vector for each bin of the standard session was then correlated with the firing rate vector for each bin of the mismatch session to produce a STD versus MIS correlation matrix (Fig. 3; Supplementary Fig. 2). For the 45° mismatch sessions, the STD versus MIS matrices for both CA1 and CA3 showed a large correlation on the diagonal, indicating that both regions maintained strong coherence in their representations between the standard and mismatch sessions with the smallest mismatch angle tested (compare with the correlation matrices between the standard 1 and standard 2 sessions). When the mismatch angles were greater than 45°, the CA1 representations lost their coherence between the standard and mismatch sessions, as the diagonal band of high correlation disappeared. In contrast, CA3 maintained a structured, diagonal band of highly correlated activity in all mismatch types. As the mismatch angle increased, the band of high correlation shifted downward, consistent with the observation that the majority of CA3 place fields rotated ACW with the local cues.

We used circular statistics[17] to analyse the subgroup of cells that maintained place fields in both the standard and mismatch sessions. Figure 4a shows the amount that each place field rotated between
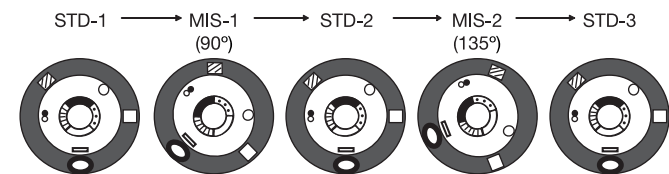

Figure 1 Experimental design. The ring track (centre) with distinctive local cues on its surface was positioned in a curtained environment (black outer circle). Distal cues were positioned along the curtained wall. Each day, the standard session (STD) was repeated three times, interleaved with cue-mismatch sessions (MIS) of different mismatch amounts (90° and 135° in this example).

the two sessions and the mean vector for each mismatch amount. The angle of the vector denotes the mean angle that the population rotated, and the length of the vector is inversely proportional to the variance of the distribution around that mean. For CA3, all mismatch amounts produced a significant vector length, indicating that the place field rotation angles were significantly clustered around the mean angle (Fig. 4a, Supplementary Fig. 3b; Rayleigh test, $P < 0.0001$). For CA1, in contrast, only the 45° and 90° mismatch sessions produced a significant vector length (Fig. 4a, Supplementary Fig. 3b; Rayleigh test, $P < 0.0001$). The CA1 cells were not randomly distributed, however (Rao's spacing test[17], $P < 0.01$ for the 45°, 90° and 135° mismatch sessions; $P < 0.05$ for the 180° mismatch session); rather, there was a bimodal distribution, as roughly equivalent numbers of place fields rotated CW and ACW with their respective cue sets (Fig. 4a).

Because the preceding analyses combined data from multiple sessions over all 5 rats, the results may be an artefact of combining these different data sets. That is, it is possible that CA1 and CA3 maintained an equivalent amount of coherence in individual, simultaneously recorded data sets, but that the CA3 ensemble

always rotated ACW whereas the CA1 ensemble sometimes rotated CW and other times rotated ACW. Combining these heterogeneous data sets would lead to an incorrect conclusion that the CA3 ensemble was internally more coherent than the CA1 ensemble. To address this possibility, we calculated the mean rotation vector for each individual data set in which at least 2 cells from both CA1 and CA3 maintained a place field in the standard and mismatch sessions (for example, see data for single data sets in Fig. 4b). A Wilcoxon signed rank test (the non-parametric analogue of a paired t-test) demonstrated that on average, the mean vector length of CA3 was greater than the mean vector length of simultaneously recorded CA1 cells ($P < 0.02$), verifying that the CA3 representation was more coherent than CA1 at the level of individual ensemble recordings (Fig. 4c).

One potential explanation for the different responses of CA3 and CA1 to the altered environments is that most CA3 place cells received inputs only from neurons that represent local cues, whereas CA1 cells received inputs from neurons that represent both local and distal cues. A number of lines of evidence argue against this interpretation: (1) although the majority of CA3 place fields rotated
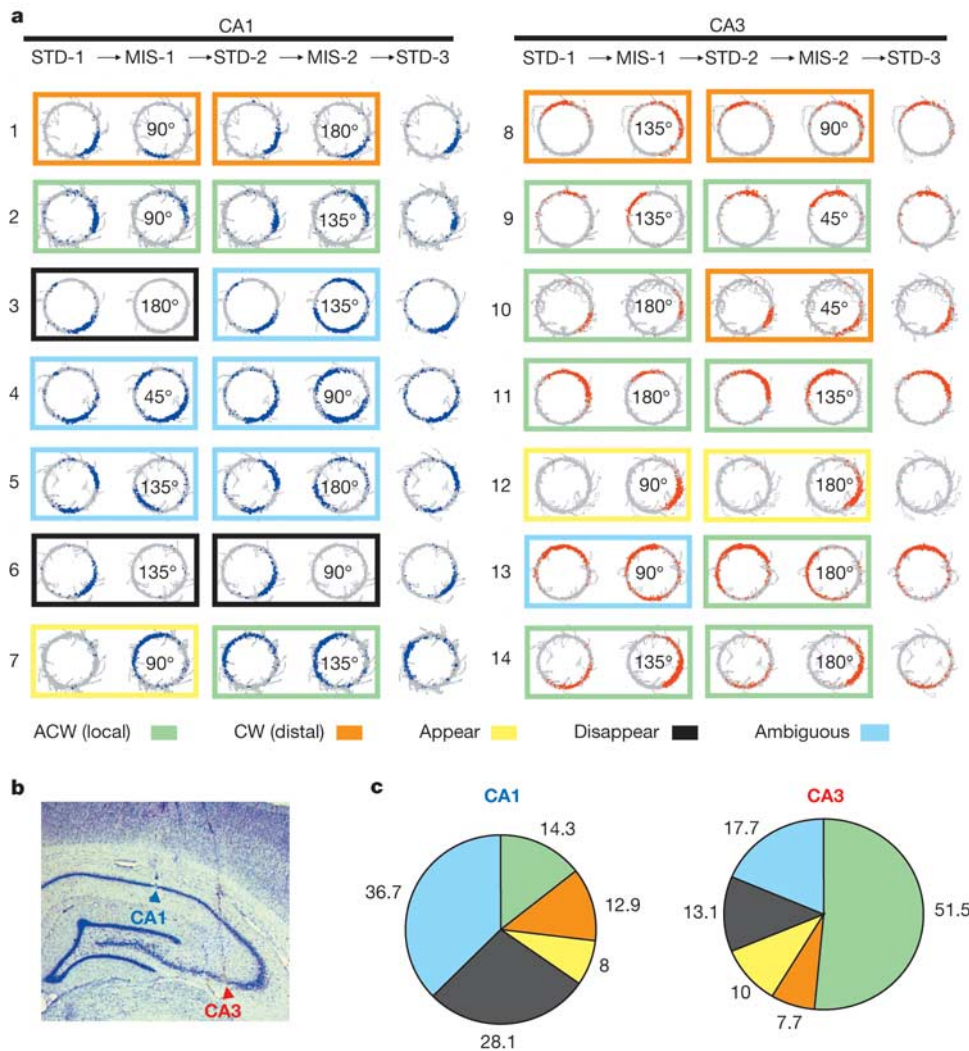

Figure 2 Individual place field responses to cue manipulations. **a**, Examples of CA1 and CA3 place fields between standard (STD) and mismatch (MIS) sessions. Each row shows five consecutive sessions in a day. Rectangles of different colours denote five response categories. Position data are shown as grey dots, and spikes as coloured dots. Angles denote mismatch amount between local and distal cue sets. These examples of place cells were not recorded simultaneously. **b**, Representative locations of CA1 (blue arrowhead) and CA3 (red arrowhead) electrodes within a subject. **c**, Categorical classification of place field behaviour in response to mismatch sessions. Numbers show per cent.

©2004 **Nature Publishing Group**

with the local cues, almost half of the place fields rotated with the distal landmarks, remapped or behaved ambiguously. Moreover, some individual CA3 place fields were controlled by the local cues in one session and by the distal cues in another session (for example, Fig. 2a, cell 10). (2) The CA3 place fields that rotated ACW tended to rotate by a lesser amount than the local cues themselves, and this under-rotation was greater and more variable for the 180° mismatch session than for the 45° mismatch session (Fig. 4d; $P < 0.02$ between the 45° and 180° conditions, Kolmogorov-Smirnov test; see also Supplementary Fig. 4). This result demonstrates an interaction between both sets of cues in CA3. (3) A preliminary study in one of the present subjects showed that CA3 place fields were more highly correlated than CA1 place fields when distal landmarks alone were rearranged, in a situation in which the local cues were removed (Supplementary Figs 5 and 6). These data are in agreement with prior studies that showed that CA3 place fields were controlled by rotations of distal landmarks as robustly as CA1 place fields[18,19]. Despite the evidence showing modulation of CA3 place fields by distal cues, it is still possible that CA3 is more dominantly influenced by local cues than is CA1 (especially when there is a competition between local and distal cues[15]). Recordings from the brain structures that send inputs to CA3 and/or CA1 (for example, the entorhinal cortex and the dentate gyrus) will be necessary to test this hypothesis rigorously. Nevertheless, the present data clearly show that neurons in CA3 respond to the altered environments in a more coherent fashion than CA1 neurons.

Since the pioneering theories of Marr[6], the hippocampus is often modelled as an autoassociative memory network that can retrieve the originally stored representation in the presence of incomplete, corrupt, or noisy inputs ('pattern completion' or 'generalization')[6–10,20,21]. CA3 is thought to perform such autoassociative functions via its recurrent collateral circuitry[4–12]. Consistent with those theories, the present study provides (to our knowledge) the first direct electrophysiological evidence in normal animals

that CA3 displays far more homogeneity in its ensemble response to an altered environment than CA1. Under different circumstances, however, it might be adaptive for a network to create a new, independent representation of an altered environment[6] (for example, if there are different behavioural contingencies associated with the familiar and altered environments). 'Pattern separation' refers to this ability of a network to make the representations of two similar input patterns more dissimilar, thus decreasing the probability of recall errors[22–25]. Most theories consider the information processing in the dentate gyrus as an essential stage for the pattern separation process[7,22–24]. The CA3 subfield, which receives a major input from the dentate gyrus via the mossy fibre projection, may be the region where the dynamic tension between these pattern completion and pattern separation processes is resolved[22,23]. Under some circumstances (such as the present study, when environmental cues are altered), the CA3 network performs a pattern completion process; under other circumstances (perhaps when the spatial landmarks or other internal variables are altered to
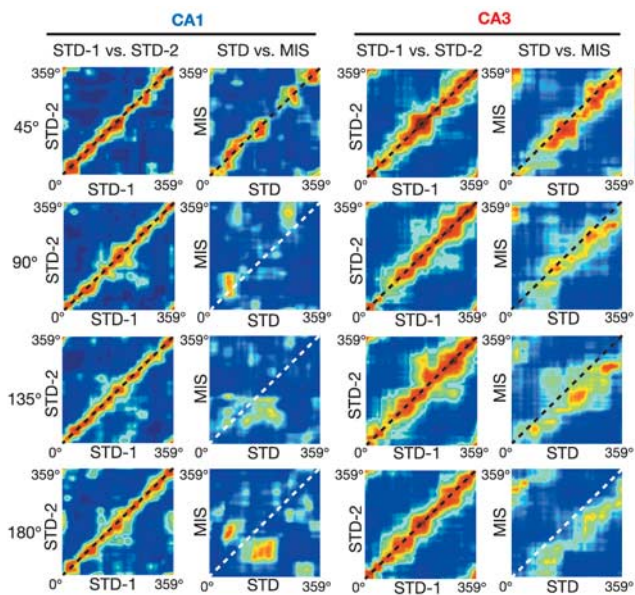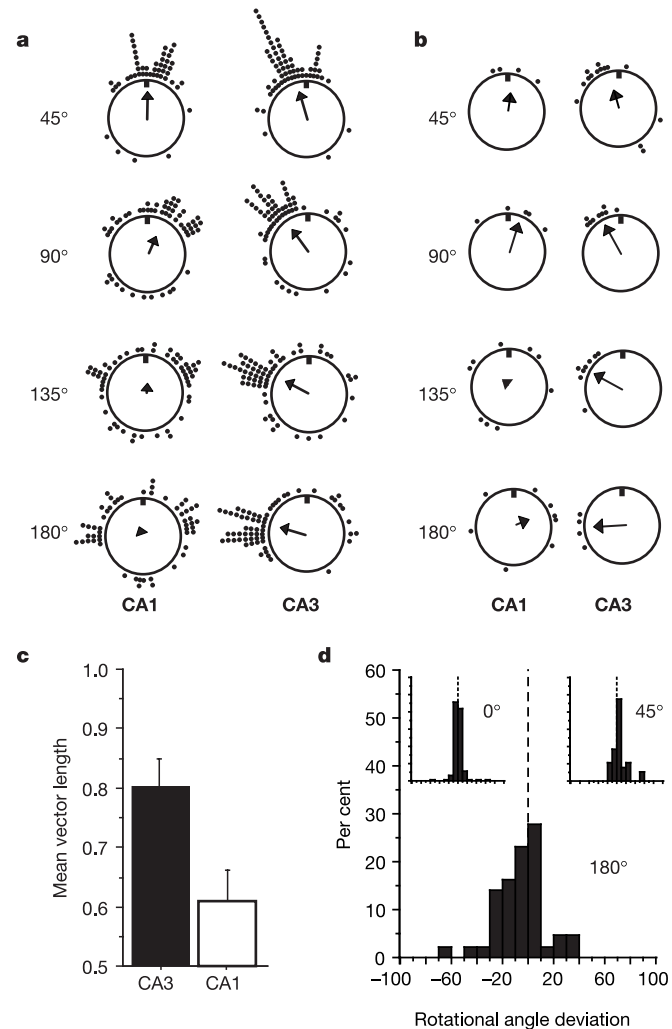

Figure 3 Correlation matrices between population firing rate vectors. Matrices shown are between population firing rate vectors of the first and the second standard sessions (STD-1 versus STD-2 correlation matrix) or between those of standard and mismatch sessions (STD versus MIS correlation matrix) for each mismatch condition. The abscissa and the ordinate represent the locations (°) on the linearized track in the standard and/or mismatch sessions. The CA3 representation remained coherent at all mismatch angles, whereas the CA1 representation abruptly lost coherence when mismatch angles exceeded 45° (see Supplementary Fig. 3a).

Figure 4 Ensemble coherence. a, Each dot represents the calculated amount of rotation of a single place field between the standard and mismatch sessions. Zero degree is denoted by the tick mark in each circle. b, Representative examples of ensembles of CA1 and CA3 place fields recorded simultaneously. c, Average vector lengths for simultaneously recorded CA1 and CA3 place field ensembles (mean ± s.e.m.).
d, Deviation of the calculated rotation angle of the ACW-rotating CA3 place fields from the physical rotation angle of the local cue set in the 180° mismatch condition, 45° mismatch condition (right inset), and standard session (left inset). Negative numbers denote under-rotation relative to the rotation of the cue set and positive numbers denote over-rotation.

a greater extent, producing a strong pattern separation via the dentate gyrus), the CA3 ensemble transitions to a completely different location (attractor) in its representation state space[13,25,26].

An important finding of the present results is that the CA1 representation was not always under the strong control of its CA3 afferents[14,25]. The role of CA1 may be to compare the rat's current experience, represented in the entorhinal inputs, with the representations of past experience stored in the DG-CA3 networks[8]. Under some circumstances, the CA1 output may be dominated by its CA3 afferents, and the CA1 and CA3 representations will behave coherently with each other (as in the 45° mismatch session; see Fig. 3). Under other circumstances, however, such as in novel environments or sufficiently altered environments (such as the larger mismatch sessions), CA1 may be dominated by its EC afferents[27] and its representation may be less strongly influenced by the CA3 output[25,28]. Recordings or manipulations specifically targeting these networks in various conditions will promote further understanding of how the interactions among these networks optimize memory storage and retrieval[10,11,22,27,29].

Note added in proof: While our paper was in production, we became aware of another study[31] (using immediate-early genes to measure activity) that reached conceptually similar conclusions about differences between CA1 and CA3. □

Methods

Detailed experimental procedures were described previously[16]. All animal procedures were in accordance with NIH guidelines on the use of experimental animals and were approved by the University of Texas Health Science Center at Houston Institutional Animal Care and Use Committee. Twelve tetrodes were lowered to CA3, and 6 tetrodes were lowered to CA1. We specifically targeted the middle or distal CA3 region because this region provides a higher density of recurrent collaterals than the proximal CA3 region[5]. We also targeted the middle and proximal CA1 region, as this part of CA1 receives topographically organized input from the middle and distal CA3, respectively[4,5]. Only those tetrodes that allowed unambiguous assignments to either CA1 or CA3 were used for further analysis, and data from the tetrodes in CA2 or the hilar area were discarded. After a week of recovery from electrode implant surgery, the rats were trained (7–13 days) to circle clockwise (CW) on a circular track (56 cm inner diameter, 76 cm outer diameter) to collect chocolate reward placed on random locations of the track. During the course of training before recording place fields, the animals were trained to run only clockwise. Whenever the rat turned around and moved anticlockwise (ACW), its progress was stopped by blocking its path with a paper folder. The rats quickly learned to move unidirectionally in a clockwise direction. The experimenter was present in the testing room at the time of recording and, when the rat occasionally turned around to run anticlockwise, the experimenter corrected the behaviour. The track was composed of 4 different textured surfaces ('local cues'), each covering one-quarter of the ring: a grey rubber mat with a pebbled surface, brown medium-grit sandpaper, beige carpet pad material, and grey duct tape with white tape stripes. The track was placed in a circular, curtained environment (2.7 m diameter) in which six objects ('distal cues') were present either on the floor or on the curtain ('hanging cues'—a brown cardboard circle, a black and white striped card, and a white card; 'standing cues'—a white box, an intravenous stand with a laboratory coat and a blue cloth, and a roll of brown wrapping paper).

Multiple single units were recorded with the Cheetah data acquisition system (Neuralynx), and the animal's position was monitored at 30 Hz via an array of light-emitting diodes mounted on the headstage. Once the testing started, each animal was given baseline sleep periods (~30 min), during which multiple cells were recorded, before the first behavioural testing session and after the last testing session. These sleep data were used to determine the stability of recordings made during behavioural sessions and unstable cells were not further analysed.

After perfusion, electrode tracks were histologically identified and the tetrodes were carefully assigned to subfields of the hippocampus by considering both histological results and electrophysiological profiles of the tetrodes recorded during the experiments. Specifically, digital photomicrographs were taken for all serial sections of the hippocampus (40 μm). Tetrode tracks were traced on the digital images using graphic software (Adobe) and those retouched images were reconstructed three-dimensionally (Voxar). Microscopic examinations were used in parallel in the course of reconstruction. Rotated three-dimensional views of the reconstructed three-dimensional image were compared to the configuration of the tetrodes in the original tetrode-bundle for accurate identification of the tetrodes.

Units were isolated off-line using custom software for cluster cutting. The track was divided into 360 bins (1° per bin) and a firing rate for each bin was calculated by dividing the number of spikes fired while the rat occupied that bin by the amount of time spent in the bin. The place fields were smoothed by a gaussian filter with width parameter $\sigma = 4.3°$. The amount that each place field rotated between the standard and mismatch sessions was calculated by computing the Pearson product-moment correlation between its firing rate array for the standard session and for the mismatch session; the latter session was shifted successively by 1° until the maximum correlation between the two arrays was found. This correlational analysis to find rotation angles was performed only when well-established place fields (statistically significant, spatial information score[30] ≥0.5, and number of spikes ≥50) were exhibited in both standard and mismatch sessions.

1. O'Keefe, J. & Nadel, L. *The Hippocampus as a Cognitive Map* (Clarendon, Oxford, 1978).
2. Eichenbaum, H. A cortical-hippocampal system for declarative memory. *Nature Rev. Neurosci.* **1**, 41–50 (2000).
3. Vargha-Khadem, F. *et al.* Differential effects of early hippocampal pathology on episodic and semantic memory. *Science* **277**, 376–380 (1997).
4. Amaral, D. G. & Witter, M. P. in *The Rat Nervous System* (ed. Paxinos, G.), 2nd edn 443–493 (Academic, San Diego, 1995).
5. Ishizuka, N., Weber, J. & Amaral, D. G. Organization of intrahippocampal projections originating from CA3 pyramidal cells in the rat. *J. Comp. Neurol.* **295**, 580–623 (1990).
6. Marr, D. Simple memory: a theory for archicortex. *Phil. Trans. R. Soc. Lond.* **262**, 23–81 (1971).
7. Rolls, E. T. & Treves, A. *Neural Networks and Brain Function* (Oxford Univ. Press, Oxford, 1998).
8. Hasselmo, M. E., Schnell, E. & Barkai, E. Dynamics of learning and recall at excitatory recurrent synapses and cholinergic modulation in rat hippocampal region CA3. *J. Neurosci.* **15**, 5249–5262 (1995).
9. McNaughton, B. L. & Morris, R. G. M. Hippocampal synaptic enhancement and information storage within a distributed memory system. *Trends Neurosci.* **10**, 408–415 (1987).
10. Kesner, R. P. & Rolls, E. T. Role of long-term synaptic modification in short-term memory. *Hippocampus* **11**, 240–250 (2001).
11. Nakazawa, K. *et al.* Requirement for hippocampal CA3 NMDA receptors in associative memory recall. *Science* **297**, 211–218 (2002).
12. Treves, A. & Rolls, E. T. Computational analysis of the role of the hippocampus in memory. *Hippocampus* **4**, 374–391 (1994).
13. Samsonovich, A. & McNaughton, B. L. Path integration and cognitive mapping in a continuous attractor neural network model. *J. Neurosci.* **17**, 5900–5920 (1997).
14. McNaughton, B. L., Barnes, C. A. & O'Keefe, J. The contributions of position, direction, and velocity to single unit activity in the hippocampus of freely-moving rats. *Exp. Brain Res.* **52**, 41–49 (1983).
15. Shapiro, M. L., Tanila, H. & Eichenbaum, H. Cues that hippocampal place cells encode: dynamic and hierarchical representation of local and distal stimuli. *Hippocampus* **7**, 624–642 (1997).
16. Knierim, J. J. Dynamic interactions between local surface cues, distal landmarks, and intrinsic circuitry in hippocampal place cells. *J. Neurosci.* **22**, 6254–6264 (2002).
17. Zar, J. H. *Biostatistical Analysis*, 4th edn (Prentice Hall, Upper Saddle River, NJ, 1999).
18. O'Keefe, J. & Speakman, A. Single unit activity in the rat hippocampus during a spatial memory task. *Exp. Brain Res.* **68**, 1–27 (1987).
19. Cressant, A., Muller, R. U. & Poucet, B. Remapping of place cell firing patterns after maze rotations. *Exp. Brain Res.* **143**, 470–479 (2002).
20. Hopfield, J. J. Neural networks and physical systems with emergent collective computational abilities. *Proc. Natl Acad. Sci. USA* **79**, 2554–2558 (1982).
21. Mizumori, S. J., McNaughton, B. L., Barnes, C. A. & Fox, K. B. Preserved spatial coding in hippocampal CA1 pyramidal cells during reversible suppression of CA3c output: evidence for pattern completion in hippocampus. *J. Neurosci.* **9**, 3915–3928 (1989).
22. Kesner, R. P., Gilbert, P. E. & Wallenstein, G. V. Testing neural network models of memory with behavioral experiments. *Curr. Opin. Neurobiol.* **10**, 260–265 (2000).
23. O'Reilly, R. C. & McClelland, J. L. Hippocampal conjunctive encoding, storage, and recall: avoiding a trade-off. *Hippocampus* **4**, 661–682 (1994).
24. McNaughton, B. L. & Nadel, L. in *Neuroscience and Connectionist Theory* (eds Gluck, M. A. & Rumelhart, D. E.) 1–63 (Erlbaum, Hillsdale, NJ, 1990).
25. Leutgeb, S., Kjelstrup, K. G., Treves, A., Moser, M. & Moser, E. I. *Differential Representation of Context in Hippocampal Areas CA3 and CA1* (Program No. 91.5, Abstract Viewer/Itinerary Planner, Society for Neuroscience, Washington DC, 2003).
26. Kali, S. & Dayan, P. The involvement of recurrent connections in area CA3 in establishing the properties of place fields: a model. *J. Neurosci.* **20**, 7463–7477 (2000).
27. Brun, V. H. *et al.* Place cells and place recognition maintained by direct entorhinal-hippocampal circuitry. *Science* **296**, 2243–2246 (2002).
28. Anderson, M. I. & Jeffery, K. J. Heterogeneous modulation of place cell firing by changes in context. *J. Neurosci.* **23**, 8827–8835 (2003).
29. Lee, I. & Kenser, R. P. Differential contribution of NMDA receptors in hippocampal subregions to spatial working memory. *Nature Neurosci.* **5**, 162–168 (2002).
30. Skaggs, W. E., McNaughton, B. L., Wilson, M. A. & Barnes, C. A. Theta phase precession in hippocampal neuronal populations and the compression of temporal sequences. *Hippocampus* **6**, 149–172 (1996).
31. Vazdjarjanova, A. & Guzowski, J. F. Differences in hippocampal neuronal population responses to modifications of an environmental context: evidence for distinct, yet complementary, functions of CA3 and CA1 ensembles. *J. Neurosci.* (in the press).